Lawrence Berkeley National Laboratory
LBL Publications

Title
A Simple, Multidimensional Approach to High-Throughput Discovery of Catalytic Reactions

Permalink
https://escholarship.org/uc/item/07q3m5zp

Journal
Science, 333(6048)

ISSN
0036-8075

Authors
Robbins, D. W.
Hartwig, J. F.

Publication Date
2011-09-09

14. A. I. R. Herries, J. Shaw, *J. Hum. Evol.* **60**, 523 (2011).
15. A. P. Roberts, *Geophys. Res. Lett.* **35**, L17307 (2008).
16. J. Woodhead *et al.*, *Quat. Geochronol.* **1**, 208 (2006).
17. R. Pickering, J. D. Kramers, T. C. P. Partridge, J. Kodolanyi, T. Pettke, *Quat. Geochronol.* **5**, 544 (2010).
18. J. E. T. Channell, A. Mazaud, P. Sullivan, S. Turner, M. E. Raymo, *J. Geophys. Res.* **107**, 2114 (2002).
19. B. A. Carlson *et al.*, *Science* **332**, 583 (2011).
20. J. M. Kibii *et al.*, *Science* **333**, 1407 (2011).
21. B. Zipfel *et al.*, *Science* **333**, 1417 (2011).
22. T. L. Kivell, *Science* **333**, 1411 (2011).

A Simple, Multidimensional Approach to High-Throughput Discovery of Catalytic Reactions

Daniel W. Robbins and John F. Hartwig*

Transition metal complexes catalyze many important reactions that are employed in medicine, materials science, and energy production. Although high-throughput methods for the discovery of catalysts that would mirror related approaches for the discovery of medicinally active compounds have been the focus of much attention, these methods have not been sufficiently general or accessible to typical synthetic laboratories to be adopted widely. We report a method to evaluate a broad range of catalysts for potential coupling reactions with the use of simple laboratory equipment. Specifically, we screen an array of catalysts and ligands with a diverse mixture of substrates and then use mass spectrometry to identify reaction products that, by design, exceed the mass of any single substrate. With this method, we discovered a copper-catalyzed alkyne hydroamination and two nickel-catalyzed hydroarylation reactions, each of which displays excellent functional-group tolerance.

Mechanistic data often provide the foundation for catalyst development and optimization. However, many reactions were discovered serendipitously while seeking a different synthetic transformation (*1*, *2*). The advent of combinatorial methods for the discovery of new drug candidates and new enzymes for organic synthesis has raised the prospect of applying analogous high-throughput experimental methods to the discovery of catalytic transformations. Many studies on this topic have been published over t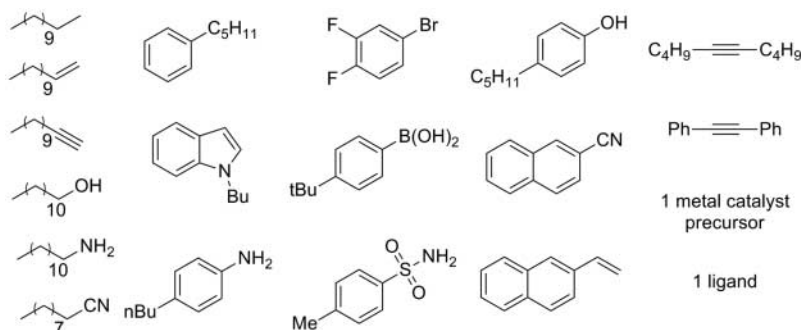he past two decades (*3–17*). Although the experimental designs that have been reported all have merit, few have been used by laboratories beyond those disclosing the original studies. Many of these approaches require cationic intermediates (*11*, *12*, *15*, *16*), acidic products (*18*), substrates with colorimetric tags, serial optimization of portions of modular ligands (*19–21*), the attachment of reactants to DNA fragments and polymerase chain reaction amplification to identify the product, or robotic equipment with a cost that is prohibitory to most laboratories. Thus, to apply combinatorial methods to catalyst discovery in a general fashion, new methods that require equipment commonly available in a synthetic laboratory or obtainable at a comparable cost are needed.

Most published methods for the high-throughput discovery of catalysts evaluate one of the two catalyst-reactant dimensions. In other words, these methods have been used to examine either many catalysts for a single class of reaction or a single catalyst for many reactions.

Department of Chemistry, University of Illinois, Urbana-Champaign, Urbana, IL 61801, USA.

*To whom correspondence should be addressed. E-mail: jhartwig@illinois.edu

Fig. 1. Contents of a single well in the multidimensional experiments for reaction discovery. The combination of 17 substrates was placed into each reaction well. Twelve ligands were dispensed, one into each well of a column, and eight metal catalyst precursors were dispensed, one into each well of a row. The plate was sealed and heated at 100°C for 18 hours. After this time, the contents of the wells in the plate were analyzed by mass spectrometry. The number of substrates is arbitrary; the 17 substrates contain a representative set, not a comprehensive set, of typical organic functional groups. A group of catalysts derived from Mn, Fe, Cr, Co, Cu, Ni, and W was chosen because of its abundance and low cost. In addition, we examined catalysts derived from Ru and Mo because these are inexpensive relative to the more precious metals, Yb as a representative f-block metal, and Au because of its wide range of reactivity that has recently been uncovered. The ligands we combined with these metals included common phosphines and amines, as well as less explored phosphine oxides, phosphine sulfides, and amidinates (table S1). Excess of the metal complexes were used in this system to alleviate poisoning all of the potential catalysts by one substrate. Reactions discovered in such a system would be rendered catalytic after initial identification of the transformation and metal-ligand combination that induces the transformation. The 17 substrates, in combination with catalysts derived from 15 metal centers and 23 ligands or the absence of a ligand, correspond to more than 50,000 reactions. These reactions were conducted in a few days, after developing our protocol. Bu, butyl; tBu, tert-butyl; Me, methyl; Ph, phenyl.

A two-dimensional approach in which many catalysts for many possible catalytic reactions are tested simultaneously would create a more efficient discovery platform if the reactants and products from such a system could be identified. Here, we disclose a method to discover catalytic reactions by conducting experiments in an *xy* array on pools of substrates that have similar masses and analyzing combinations of these pools by mass spectroscopy. This format allows us to evaluate thousands of reactions at one time and to pinpoint, with just a few mass spectral measurements, the coordinates of the metal and ligand that effect a reaction between two or more substrates.

For the study described here, we conducted the core experiment with a set of 17 organic reactants, each of which contains 10 to 13 heavy atoms (C, N, O, F, S) and possesses a single functional group (Fig. 1) (22). A reaction between two of these substrates would produce a product with a mass outside of the range of masses of the reactants. We obtained mass spectral data by a combination of gas chromatography–mass spectrometry (GC-MS) to measure the masses of nonpolar products and electrospray ionization mass spectrometry (ESI-MS) to measure the masses of polar products (23). The mass of potential products from joining two substrates is easily calculated from the masses of the reactants, including the masses of potential products formed with concomitant loss of common small molecules, such as H_2O, NH_3, H_2, and HCN or common leaving groups, such as halides (24).

We chose the catalyst components for the initial implementation of this strategy to identify Earth-abundant metals that catalyze reactions previously induced by precious metal complexes. Although progress has been made toward the goal of catalyzing reactions with first-row transition metals, the smaller body of mechanistic information on reactions catalyzed by such systems makes high-throughput discovery methods particularly appealing. The exact metals and ligands that we used in these experiments are depicted in table S1. The reactions identified in this format would necessarily have the high degree of functional-group tolerance most often needed to prepare natural products and medicinally important compounds (22), because they were formed in a medium containing a wide range of additional functional groups.

To minimize the number of mass spectra, in anticipation of conducting such studies on a large format, we analyzed reaction products by creating 8 samples containing a portion of the contents of each row and 12 samples containing a portion of the contents of each column of a 96-well plate. By this method, only 20 mass spectra on each 96-well plate are needed to identify the *xy* coordinates of the metal-ligand combination that gives rise to a reaction product. These coordinates correspond to the pooled samples of the row and column containing the same reaction product. In some cases, the product (and, there-

fore, the reaction partners) would be difficult to determine from the mass spectrum alone. Therefore, we devised an additional protocol to identify the product within a particular well by running a small set of additional experiments (see below).

We implemented our design by conducting experiments in which the 17 reagents were combined in each of 384 wells (of a 16-by-24 array), with all but one well containing one metal pre-

cursor (15 total plus 1 negative control containing no metal) and one ligand (23 ligands plus 1 negative control containing no ligand). In this experiment, we included the substrates, metal-catalyst precursors, and ligands for three known reactions as positive controls. These reactions were the Ni-catalyzed carbocyanation of an alkyne (25), the Cu-catalyzed oxidative coupling of an aromatic amine and an aryl boronic acid (26), and the Ru-catalyzed alkylation of a sulfonamide
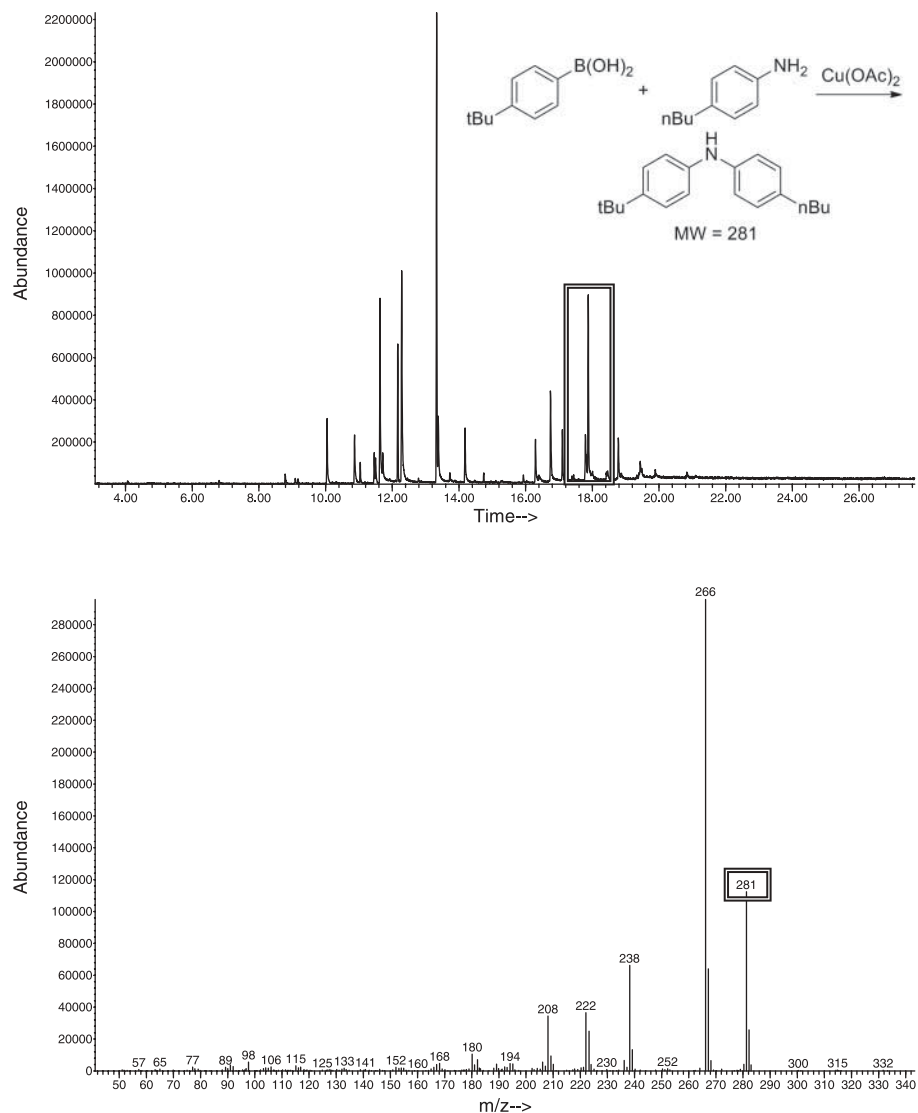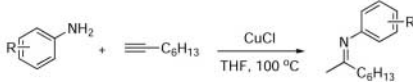
Fig. 2. GC–mass spectrum of the combination of reactions in the row containing $Cu(OAc)_2$ as a metal catalyst precursor. The product from Cu-catalyzed oxidative coupling was observed. The peak at 17.9 min corresponds to material with an *m/z* value of 281, which is the mass of the amination product. MW, molecular weight.
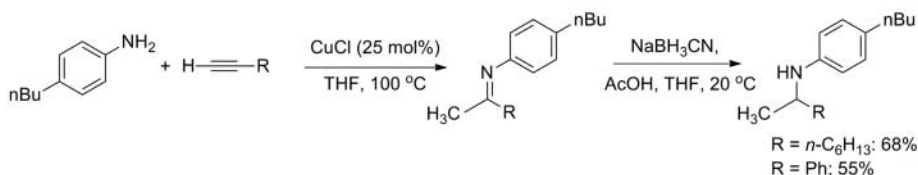
Fig. 3. Cu-catalyzed alkyne hydroamination with 4-*n*Bu-aniline. THF, tetrahydrofuran.

Table 1. Selected copper-catalyzed alkyne hydroaminations with aromatic amines.

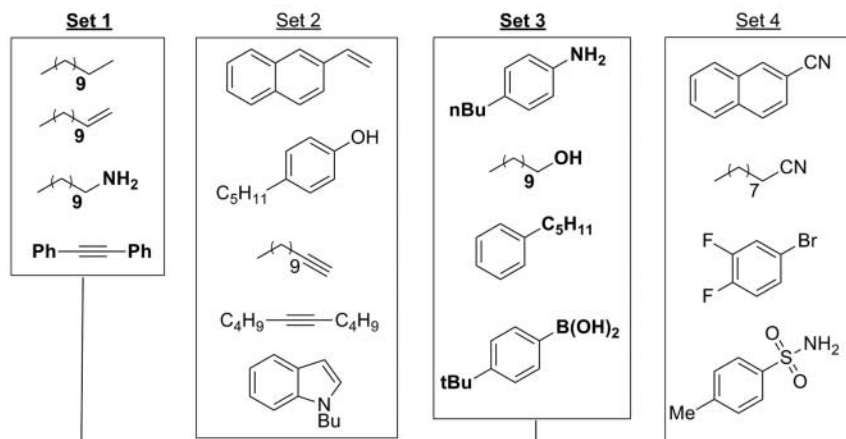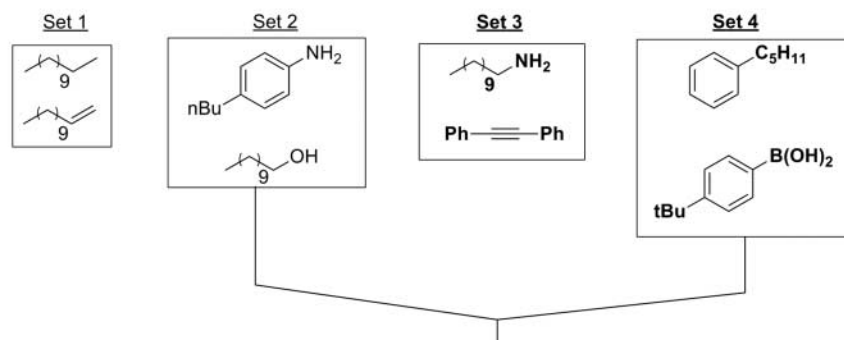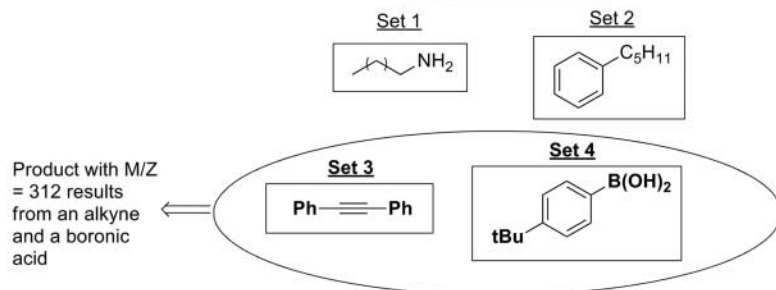| Entry	R	Catalyst Loading	Yield*
1	4-nBu	10 mol%	57%
2	4-OH	25 mol%	80%
3	4-CN	25 mol%	51%
4	4-CO₂Me	25 mol%	68%
5	3-Br	25 mol%	84%
6	4-acetyl	25 mol%	60%
7	2,6-di-isopropyl	25 mol%	70%

* Yield determined by using gas chromatography with 1,3,5-trimethoxybenzene as an internal standard after hydrolysis with 1 M HCl at room temperature to 2-octanone

Fig. 4. Deconvolution strategy to identify coupling partners for products observed in high-throughput reaction discovery.

with an alcohol (Fig. 2 and figs. S1 and S2) (27). We observed the product from each of these three reactions among the more than 50,000 possible catalytic reactions [(17·16/2 cross-combinations of substrates plus 17 homo-coupling of substrates) by 15 metal catalyst precursors by 24 ligands]. The GC-MS trace from the row containing Ni(cod)₂ (cod, 1,5-cyclooctadiene) revealed the product from carbocyanation of 5-decyne with 2-cyanonaphthalene, which eluted at 18.1 min and showed a molecular ion with a mass/charge ratio (m/z) of 291 (fig. S1). The GC-MS trace from the row containing Cu(OAc)₂ (OAc, an acetoxy group) revealed the diarylamine obtained from oxidative coupling of 4-tert-butylphenylboronic acid with 4-butylaniline, which eluted at 17.9 min and showed a molecular ion with an m/z value of 281 (Fig. 2). Finally, the ESI-MS for the row containing [Ru(p-cymene)Cl₂]₂ [cymene, 1-methyl-4-(1-methylethyl)benzene] had peaks corresponding to the mono- and dialkylation of p-toluenesulfonamide with 1-dodecanol (fig. S2) with m/z = 339 and m/z = 507, respectively. These positive-control experiments showed that discrete transition metal–catalyzed reactions can be identified from a pool of substrates that could undergo thousands of possible binary reactions.

In addition to the products of these positive-control reactions, we observed the products from a reaction catalyzed by a first-row metal complex without ligands and a reaction catalyzed by a first-row metal complex containing a phosphine ligand. The GC–mass spectra of the solutions in the two rows containing CuCl and Cu(OAc)₂ consisted of a peak corresponding to a molecular ion with m/z = 315 (fig. S3). This product corresponds to that from the coupling of 1-dodecyne with 4-butylaniline. This peak also appeared in the GC–mass spectra of the contents of the rows corresponding to reactions containing PBu₃ (C), the β-diketiminate ligand (L), and tri-p-tolylphosphite (S), as well as the row corresponding to reactions containing no ligand (T), indicating that the reaction occurs with the copper precursors alone and with the combination of the precursors and two of the phosphine ligands or the β-diketiminate ligand.

Separate experiments with the amine, alkyne, and catalyst components alone demonstrated that the reaction of the aromatic amine with the alkyne catalyzed by CuCl and Cu(OAc)₂ leads to the Markovnikov addition of the amine to the alkyne, followed by tautomerization to the corresponding imine (Fig. 3) (28, 29–31). The product of this reaction was isolated as the secondary amine after reduction with NaBH₃CN. Reactions catalyzed by CuCl occurred in higher yield than those catalyzed by Cu(OAc)₂ (32). Although this reaction occurs in the presence of three of the ligands identified in the combinatorial format, the reaction also proceeded rapidly in the absence of a ligand. This copper-catalyzed reaction represents a rare hydroamination of an alkyne catalyzed by a first-row metal (33–35). As shown by data in Table 1, this process occurs under conditions
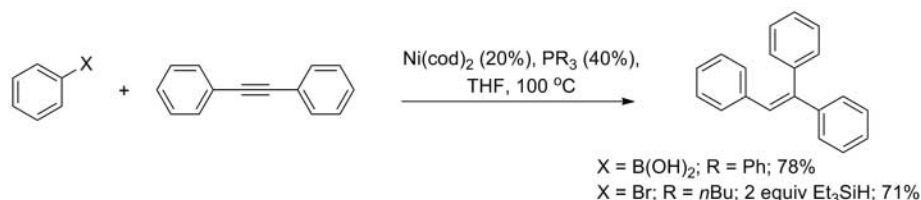
Fig. 5. Ni-catalyzed hydroarylation of diphenylacetylene with phenylboronic acid and bromobenzene.

Fig. 6. Nickel-catalyzed al-kyne hydroarylation with aryl and heteroaryl boronic acids. The ratio given is cis/trans (Z/E) olefin geometry.
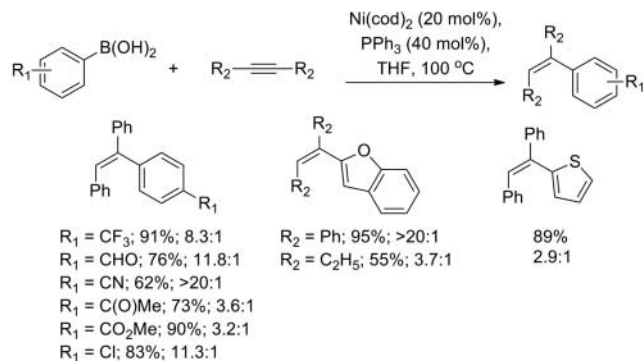
Fig. 7. Nickel-catalyzed al-kyne hydroarylation with aryl and heteroaryl bromides. The ratio given is Z:E olefin geometry. Et, ethyl.
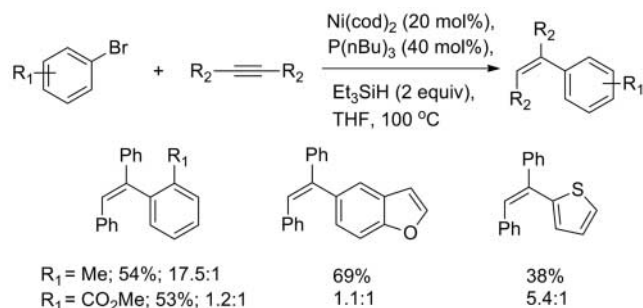
with 25 mole percent of the inexpensive CuCl in good yield. Moreover, this reaction tolerates an array of potentially reactive functional groups, such as nitriles, esters, ketones with enolizable hydrogens, and unprotected alcohols, vindicating a core hypothesis of our experimental design.

The GC-MS analysis from our experiment also revealed a reaction product eluting at 18.6 min with an apparent molecular ion having an m/z value of 312. This peak was observed in the traces of the wells containing the combination of Ni(cod)$_2$ or NiCl$_2$-dme (dme, 1,2-dimethoxyethane) and several phosphine ligands and an N-heterocyclic carbene (fig. S4). Because the identity of this product was not obvious from the mass spectrum, we devised a deconvolution strategy to determine the reactants from which it formed.

For this strategy, we first divided the potential reactants (in this case, 17) into a small number of subsets (in this case, three sets of 4 potential reactants and one set of 5 potential reactants) (Fig. 4 and figs. S15 to S18) And then combined the reactants in each of these sets to create four reactant pools. The pool of reactants in one set was then allowed to react with the three other

pools in the presence of the metal catalyst precursor and ligand that had been shown to form the unidentified product. These binary combinations of the four sets of substrates corresponded to just six reactions. In addition, to assess whether the coupling of two of the reactants requires a third component that could act as a ligand or promoter, three of the substrate sets were also allowed, in parallel, to react in a similar manner, for a total of 10 reactions. This set of 10 reactions identified the two sets that contained the reactants that formed the unknown product. We then divided the components of these two sets into four sets, each containing two substrates. In a similar manner, we conducted 10 reactions in parallel with the metal catalyst precursor and ligand and identified the two sets that yielded the desired product. We then allowed the four individual components of these sets to react with each other in binary and ternary combinations. From these reactions, we identified the two reactants that formed the unknown product.

This short series of 3 by 10 reactions showed that the unknown product with $m/z = 312$ corresponded to the hydroarylation of diphenylacetylene with 4-tert-butylphenylboronic acid to yield a

triarylalkene product. A similar strategy showed that an additional product in the wells containing Ni(cod)$_2$ and P(nBu)$_3$ that eluted at 16.6 min with a molecular ion of $m/z = 292$ (fig. S5) corresponded to a triarylalkene product from hydroarylation of diphenylacetylene with the haloarene 4-bromo-1,2-difluorobenzene. Examination of the combinations of Ni(cod)$_2$ and NiCl$_2$-dme with the ligands identified from the initial catalyst screening showed that Ni(cod)$_2$ and PPh$_3$ catalyzed the hydroarylation of diphenylacetylene with phenylboronic acid to give triphenylethylene in good yield (Fig. 5). The reaction catalyzed by Ni(cod)$_2$ without an added ligand formed just 15% yield of triphenylethylene. When the hydroarylation of diphenylacetylene was conducted with bromobenzene and the combination of Ni(cod)$_2$ and P(nBu)$_3$ as the catalyst, triphenylethylene was formed in less than 10% yield, but the same reaction with triethylsilane as a third component to act as a reducing agent furnished triphenyl-ethylene in 71% yield (Fig. 5). This transformation of arylboronic acids has been reported most commonly with rhodium (36) and palladium (37) catalysts (38), which contain costly precious metals.

The synthesis of stereochemically defined trisubstituted alkenes is a challenging problem (39, 40). Such products are often prepared by stereocontrolled additions to alkynes, but fewer reactions yield anti-addition products than syn-addition products, and hydroarylations that give anti-addition products are unknown. In contrast to this precedent, the major products of the two types of nickel-catalyzed hydroarylation discovered here result from anti-addition to the alkyne in most cases (41). For example, the hydroarylation of diphenylacetylene with 4-tert-butylphenylboronic acid gave the addition product with an 8.7/1 ratio when the catalyst contained PPh$_3$. Likewise, the products from nickel catalyzed hydroarylation of an alkyne with the aryl halide and silane gave predominantly the anti-addition product. Moreover, the ligand affects the E/Z ratio from reaction of the arylboronic acid. Reactions conducted with the catalyst generated from PCy$_3$ (Cy, cyclohexyl) gave the addition product in a 1/3.8 ratio favoring the stereoisomer from syn addition. These stereochemical outcomes were unexpected and show the ability to use the discovery platform to identify reactions that occur with different selectivities, presumably, from mechanisms not followed by earlier catalysts.

A survey of this nickel-catalyzed hydroarylation of alkynes with various boronic acids (Fig. 6) showed that, like the hydroamination that we identified, this reaction tolerates a broad range of functional groups. The nickel-catalyzed hydroarylation of alkynes with aromatic boronic acids containing esters, nitriles, ketones with enolizable hydrogens, aryl chlorides, and aldehydes formed trisubstituted alkenes in good yield with generally good selectivity for the Z over E alkene geometry. 2-heteroaryl boronic acids,

which are unstable in many reactions (*42–45*), also underwent this process to form the corresponding product from trans-hydroheteroarylation of diphenylacetylene. Reaction of a heteroaryl boronic acid with an internal alkyne possessing alkyl substituents also formed the product of hydroheteroarylation.

Selected examples of the second type of alkyne hydroarylation that we discovered involving aryl halides and triethylsilane are shown in Fig. 7. Although further studies are needed to identify the most effective combination of catalyst and reducing agent, our current studies show that the reactions of aryl halides containing potentially reactive functional groups, as well as heteroaryl halides, form the trisubstituted alkenes with good-to-moderate selectivity for the product from formal trans-addition.

This approach to reaction discovery holds considerable potential for purposes beyond those revealed in the current work. For example, this system could be used to explore reactions with additives, such as oxidants, reductants, acids, and bases, and to explore reactions of two substrates with a third component, such as carbon monoxide or carbon dioxide. It could also be used to examine the reactivity of a single class of ligand with various organic substrates and transition metal–catalyst precursors. Thus, we anticipate that this approach to reaction discovery will provide a general and adaptable platform suitable for use by a wide range of laboratories for the discovery of a variety of catalytic reactions.

References and Notes

1. H. S. Eleuterio, *J. Mol. Catal.* **65**, 55 (1991).
2. K. Fischer, K. Jonas, P. Misbach, R. Stabba, G. Wilke, *Angew. Chem. Int. Ed. Engl.* **12**, 943 (1973).
3. J. P. Stambuli, J. F. Hartwig, *Curr. Opin. Chem. Biol.* **7**, 420 (2003).
4. J. Wieland, B. Breit, *Nat. Chem.* **2**, 832 (2010).
5. P. J. Fagan, E. Hauptman, R. Shapiro, A. Casalnuovo, *J. Am. Chem. Soc.* **122**, 5043 (2000).
6. T. R. Boussie *et al.*, *J. Am. Chem. Soc.* **125**, 4306 (2003).
7. A. B. Beeler, S. Su, C. A. Singleton, J. A. Porco Jr., *J. Am. Chem. Soc.* **129**, 1413 (2007).
8. H. Kinoshita, O. J. Ingham, W. W. Ong, A. B. Beeler, J. A. Porco Jr., *J. Am. Chem. Soc.* **132**, 6412 (2010).
9. M. W. Kanan, M. M. Rozenman, K. Sakurai, T. M. Snyder, D. R. Liu, *Nature* **431**, 545 (2004).
10. M. M. Rozenman, M. W. Kanan, D. R. Liu, *J. Am. Chem. Soc.* **129**, 14933 (2007).
11. C. Markert, P. Rösel, A. Pfaltz, *J. Am. Chem. Soc.* **130**, 3234 (2008).
12. C. A. Müller, A. Pfaltz, *Angew. Chem. Int. Ed.* **47**, 3363 (2008).
13. A. Teichert, A. Pfaltz, *Angew. Chem. Int. Ed.* **47**, 3360 (2008).
14. J. W. Szewczyk, R. L. Zuckerman, R. G. Bergman, J. A. Ellman, *Angew. Chem. Int. Ed.* **40**, 216 (2001).
15. P. Chen, *Angew. Chem. Int. Ed.* **42**, 2832 (2003).
16. C. Hinderling, P. Chen, *Int. J. Mass Spectrom.* **195-196**, 377 (2000).
17. H. M. Geysen *et al.*, *Chem. Biol.* **3**, 679 (1996).
18. G. T. Copeland, S. J. Miller, *J. Am. Chem. Soc.* **123**, 6496 (2001).
19. B. M. Cole *et al.*, *Angew. Chem. Int. Ed. Engl.* **35**, 1668 (1996).
20. K. D. Shimizu *et al.*, *Angew. Chem. Int. Ed. Engl.* **36**, 1704 (1997).
21. M. B. Francis, E. N. Jacobsen, *Angew. Chem. Int. Ed.* **38**, 937 (1999).
22. All but one of these compounds are commercially available.
23. Previously, custom mass spectrometers have been used to analyze, by tandem MS-MS methods, the activity of charged catalysts for reactions conducted in the gas phase. These examples have focused on comparing several catalysts for a single reaction, such as olefin polymerization and olefin metathesis (*15*, *16*) Mass spectrometry has also been used to analyze the binding of encoded organic ligands to biological targets (*17*). Our approach does not require such encoding.
24. We used several additional design elements, including the placement of different substituents on aryl groups to discriminate between them by their distinct mass spectral fragmentation patterns.
25. Y. Nakao, S. Oda, T. Hiyama, *J. Am. Chem. Soc.* **126**, 13904 (2004).
26. P. Y. S. Lam *et al.*, *Tetrahedron Lett.* **39**, 2941 (1998).
27. M. H. S. A. Hamid *et al.*, *J. Am. Chem. Soc.* **131**, 1766 (2009).
28. Intermolecular hydroamination of an alkyne has been reported with complexes of Group IV metals that are air-sensitive and generally suffer from poor functional-group compatibility, and it has been catalyzed by complexes of the precious metals palladium, rhodium, and gold. Classical additions of amines to alkynes are conducted with toxic mercury compounds.
29. L. Zhou, H.-F. Jiang, C.-J. Li, *Adv. Synth. Catal.* **350**, 2226 (2008).
30. J. Han, B. Xu, G. B. Hammond, *J. Am. Chem. Soc.* **132**, 916 (2010).
31. T. E. Müller, K. C. Hultzsch, M. Yus, F. Foubelo, M. Tada, *Chem. Rev.* **108**, 3795 (2008).
32. Reactions catalyzed by Cu(OAc)$_2$ yielded substantial product from Glaser coupling of the alkynes to form a diyne.
33. Examples are limited to those catalyzed by an air-sensitive titanium complex and a single example catalyzed by a zinc complex.
34. E. Haak, I. Bytschkov, S. Doye, *Angew. Chem. Int. Ed.* **38**, 3389 (1999).
35. K. Alex, A. Tillack, N. Schwarz, M. Beller, *ChemSusChem* **1**, 333 (2008).
36. T. Hayashi, K. Inoue, N. Taniguchi, M. Ogasawara, *J. Am. Chem. Soc.* **123**, 9918 (2001).
37. X. Xu *et al.*, *Tetrahedron* **66**, 2433 (2010).
38. P.-S. Lin, M. Jeganmohan, C.-H. Cheng, *Chemistry* **14**, 11296 (2008).
39. E.-i. Negishi *et al.*, *Acc. Chem. Res.* **41**, 1474 (2008).
40. E.-i. Negishi, G. Wang, H. Rao, Z. Xu, *J. Org. Chem.* **75**, 3151 (2010).
41. Aryl boronic acids containing electron-donating substituents at the 4-position give ~1:1 mixtures of stereoisomers.
42. G. A. Molander, B. Canturk, L. E. Kennedy, *J. Org. Chem.* **74**, 973 (2009).
43. D. M. Knapp, E. P. Gillis, M. D. Burke, *J. Am. Chem. Soc.* **131**, 6961 (2009).
44. T. Kinzel, Y. Zhang, S. L. Buchwald, *J. Am. Chem. Soc.* **132**, 14073 (2010).
45. K. Billingsley, S. L. Buchwald, *J. Am. Chem. Soc.* **129**, 3358 (2007).

Ice Flow of the Antarctic Ice Sheet

E. Rignot,[1,2]* J. Mouginot,[1] B. Scheuchl[1]

We present a reference, comprehensive, high-resolution, digital mosaic of ice motion in Antarctica assembled from multiple satellite interferometric synthetic-aperture radar data acquired during the International Polar Year 2007 to 2009. The data reveal widespread, patterned, enhanced flow with tributary glaciers reaching hundreds to thousands of kilometers inland over the entire continent. This view of ice sheet motion emphasizes the importance of basal-slip–dominated tributary flow over deformation-dominated ice sheet flow, redefines our understanding of ice sheet dynamics, and has far-reaching implications for the reconstruction and prediction of ice sheet evolution.

Ice velocity is a fundamental characteristic of glaciers and ice sheets that measures the rate at which ice is transported from the interior regions toward the ocean, the location of preferred channels of ice transport, and how ice mass evolves with time. Traditional measurements from ground-based stations are limited relative to the size of the continent, leading to an incomplete picture of Antarctica. Satellite radar interferometry, or InSAR, has been successfully used to map glacier flow independent of cloud cover, solar illumination, or the presence of surface features (*1*). Until now, however, the vast extent of East Antarctica, which comprises 77% of the continent, has been devoid of quality data; only a few floating ice shelves have been mapped, and comprehensive velocity mapping has been limited to the lower reaches of key outlet glaciers (*2*).

Balance velocity calculated from ice thickness, surface slope, and snow accumulation data provides insights about the potential flow pattern of the ice sheet (*3*), but the technique assumes an ice sheet in mass equilibrium, which is not correct everywhere, and that ice flows perpendicular to surface contours, which is a

[1]Department of Earth System Science, University of California Irvine, Irvine, CA 92697, USA. [2]Jet Propulsion Laboratory, California Institute of Technology, Pasadena, CA 91109, USA.

*To whom correspondence should be addressed. E-mail: erignot@uci.edu